

Design of a 5G Smartphone Antenna with Dual Band and MIMO Capabilities

Preeti Mishra¹ & Kirti Vyas²

Arya college of engineering and IT

preetimishra128@gmail.com & kirtivyas19@gmail.com

1 Abstract

A 4-element dual-band multiple-input multiple-output (MIMO) antenna for mobile devices that operates in the 5G New Radio band n79 band (4.4-5 GHz) and LTE band 46 (5.1-5.9 GHz). Two pairs of antennas are used to create the 4-element MIMO antenna, and they are symmetrically printed along the smartphone's two lengthy side-edge frames. The antenna was created on widely available, affordable, and simple to manufacture FR-4 substrate. Computer simulation technology (CST) software was used to build and Simulate the antenna. The antenna covers the two 5G New Radio bands without use of any decoupling techniques. Investigations have been done on antenna features like reflection coefficient, Radiation pattern, envelop correlation coefficient, and Efficiency. All operating frequencies showed improved impedance matching (Return Loss > 10 dB), high isolation (> 18.8 dB), high efficiency (> 60%), and low envelope correlation coefficient (ECC, 0.03). The suggested MIMO antenna left enough room inside the portable mobile device for other circuit integration and suitable for Future 5 generation smartphone.

Keywords: Smartphone Application, Dual Band, four-Element, 5G, ECC

2 Introduction

The demand for high data speeds is met by MIMO (Multiple Input, Multiple Output) technology, which increases channel capacity and spectral effectiveness [1]. Mobile devices, however, need numerous radio components to support MIMO technology. MIMO antennas are less preferable because element separation and bandwidth are constrained due to incompatibilities between the dimensions of MIMO antennas and the available room in mobile devices, which reduces transmission rates. As a consequence, in recent years, there has been a growing interest in learning how to construct wideband MIMO antennas with respectable separation in mobile devices with constrained sizes. The efficacy of the antenna has been improved using a variety of techniques. The simplest decoupling technique for mobile device MIMO antennas that are fixed is to increase the distance between them. If gain and bandwidth had to be temporarily sacrificed, however, shrinking the size of the antenna element is a way to increase physical distance within a given area. [2], [3]. To keep gain and bandwidth, another strategy is to reduce the number of antenna components nearby and increase their spatial separation. [4]–[10]. However, it accepts channel loss. Other researchers, however, were concentrating on enhancing element isolation by incorporating disconnection structures, [11]–[15] which are employed to enhance isolation. On the other hand, as new portable devices become smaller and lighter, more processing capacity is needed.[16]. The MIMO antenna system built on four components is used in 4th Generation (4G) and 4G Long Term Evolution (4G LTE) systems to achieve high data rates.

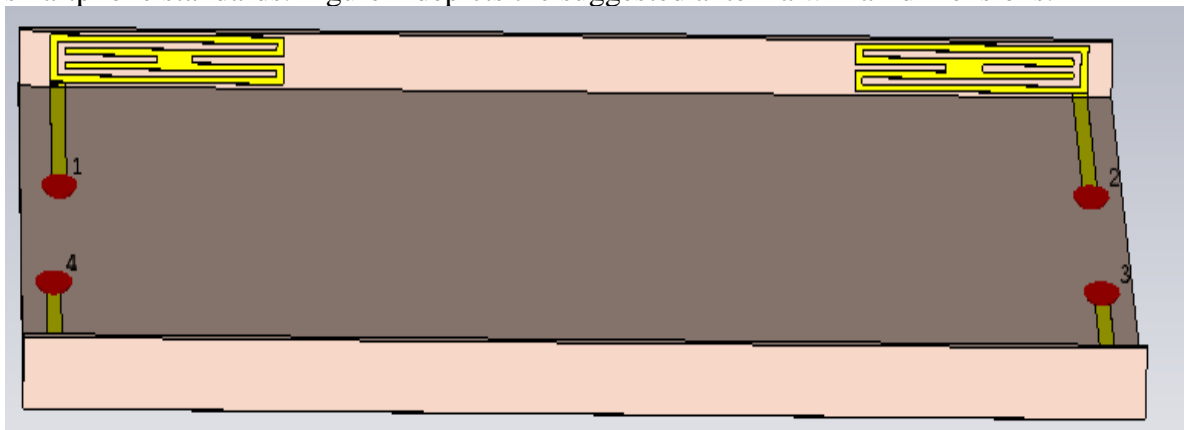
They are also widely used in contemporary wireless devices.[17], [18]. Yang et al. [17], suggested a folded box-shaped 4-element MIMO antenna for handheld LTE devices. To encourage isolation between the components, an L-branch and ground slot decoupling construction was used. This architecture complicates matters and limits the possible applications of cutting-edge technology, like 5G, in contemporary devices like tablets and cellphones. For Long Term Evolution (LTE) technology, Choi et al. suggested a 4-element reconfigurable link loop antenna device. [18].

LTE 42 and LTE 43, two of 5G frequencies, [19] correlate to a hybrid configuration with four printed components on the case's edges and corners, each with an ECC of no more than 0.3. Such hybrid structures, however, have few real-world uses due to the intricacy of the design. Thanks to the studies, various designs, components, and frames will be available for future mobile device antenna systems. (mentioned above). The most basic, low-profile, small H-shaped monopole antenna that can be used for future smartphone apps over the 5G bands between 4.4-5 GHz and 5.1-5.9 GHz is suggested by this study. In order to accomplish excellent isolation without the use of any decoupling components, the 4-port MIMO antenna system was developed.

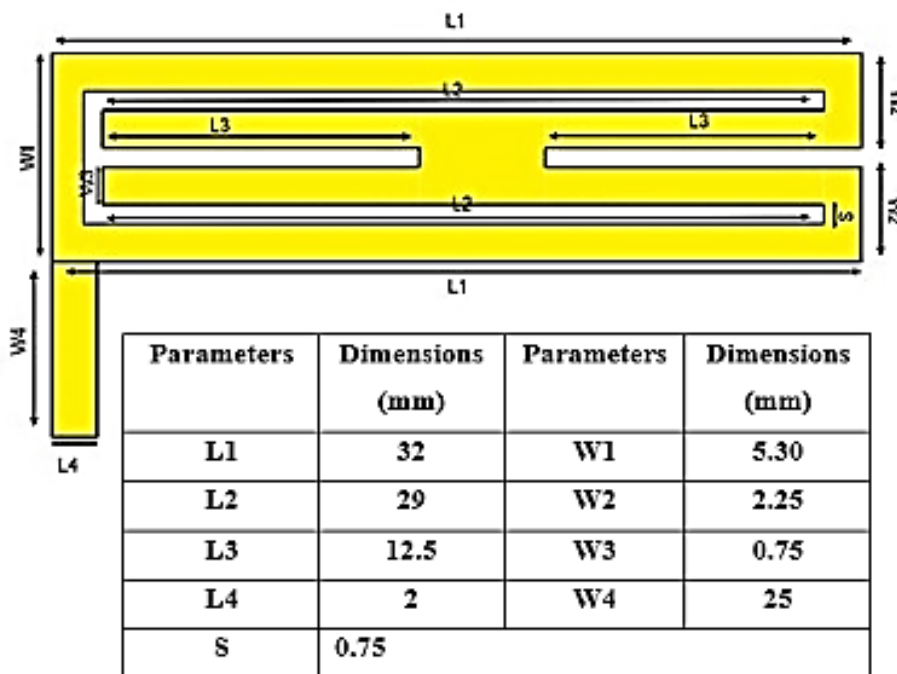
3 Antenna Design

An H-shaped monopole antenna constructed on the widely accessible, reasonably priced, and easily manufactured FR4 material. The dielectric constant and loss tangent of the material are 4.4 and 0.02, respectively. In order to achieve the size of the smartphone, the dimensions of the system substrate are 150 x 6.2 x 0.8 mm³, and two pieces of the substrate with the dimensions 150 x 6.2 x 0.8 mm, are positioned perpendicular to the substrate's length side edge. Proposed antenna elements are placed at the corner of the side rim so that there is plenty of space to connect another required circuitry. The back side of the base substrate is etched with copper to get wide-band radiation. The antenna will be fed from point 1-4. The H-shaped monopole antenna, which resonates at 4.6 GHz and 5.3 GHz, is

designed. The suggested antenna was constructed in accordance with current market smartphone standards. Figure 1 depicts the suggested antenna with all dimensions.



(a)



(b)

Figure 1: MIMO Antenna system (a) Front View (b) Dimension of the antenna

Therefore, Antenna devices used in contemporary commercial mobile phones can be confidently believed to be compatible with the suggested work. Dual-band performance at 4.6 GHz and 5.3 GHz is provided by the suggested antenna.

4 Result and Discussion

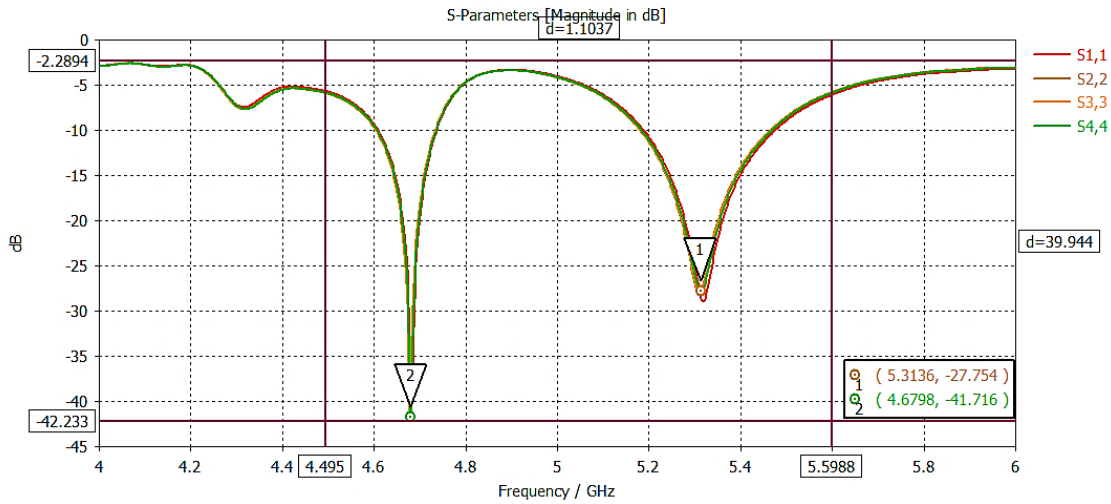
The FR4 material served as the foundation for a four-port MIMO antenna device. The performance metrics for return loss, gain, radiation pattern, and ECC are discussed in the lines that follow.

4.1 S- Parameters

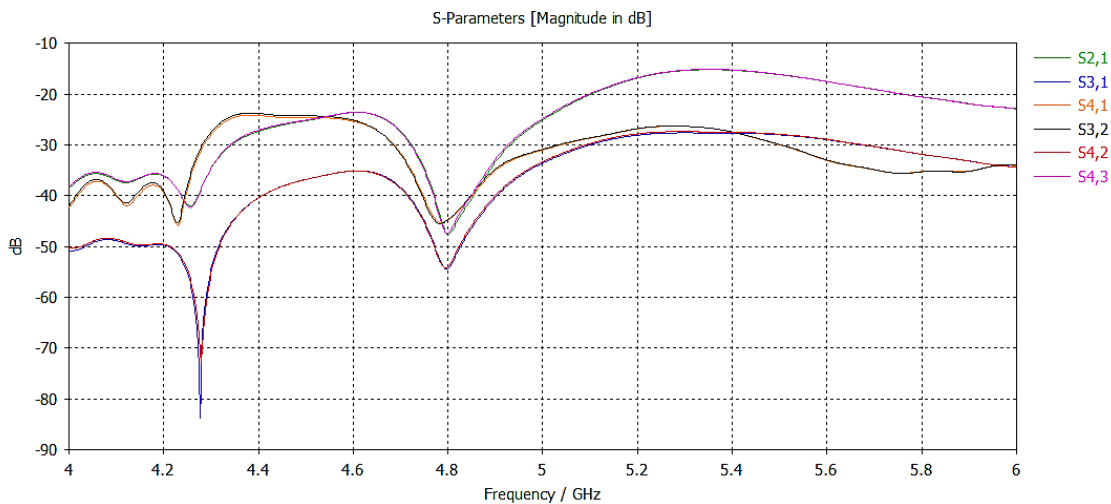
In this part, the S-parameters of the proposed antenna are discussed. In Figure 2, the refraction coefficient is displayed. It proves that the antenna can resonant

between 4.4 and 5 GHz and 5.1 and 5.9 GHz. It is significant to observe that the system is resonating at 4.6 GHz and 5.3 GHz and has -10 dB impedance.

The isolation between the antenna components is shown in Figure 3 (b). It should be noted that for both frequency bands, the distance between adjacent antenna components is greater than 12 dB. Between Ant. 1 and Ant. 4, there is a maximal isolation of > -31.8 dB and > 33.4 dB for each frequency range.



(a)



(b)

Figure 2: Scattering parameters (a) Reflection Coefficients (b) Transmission Coefficients

4.2 Antenna Efficiency

Figure 3 displays the MIMO antennas' total efficiency and radiation effectiveness. Fig. demonstrates that the radiation efficiency for both bands is 64%

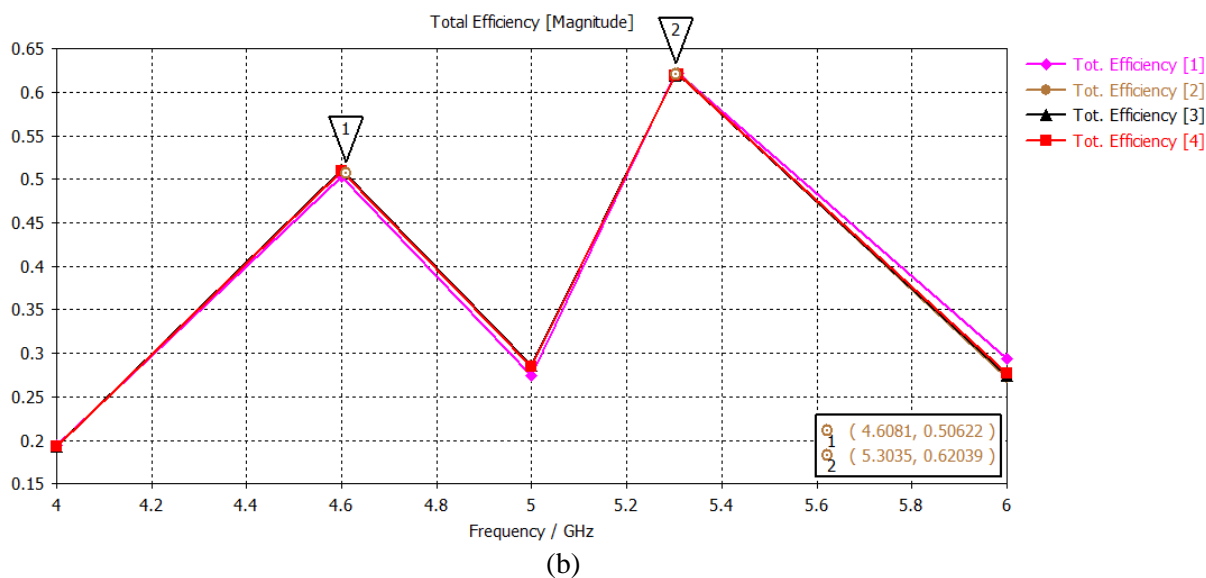
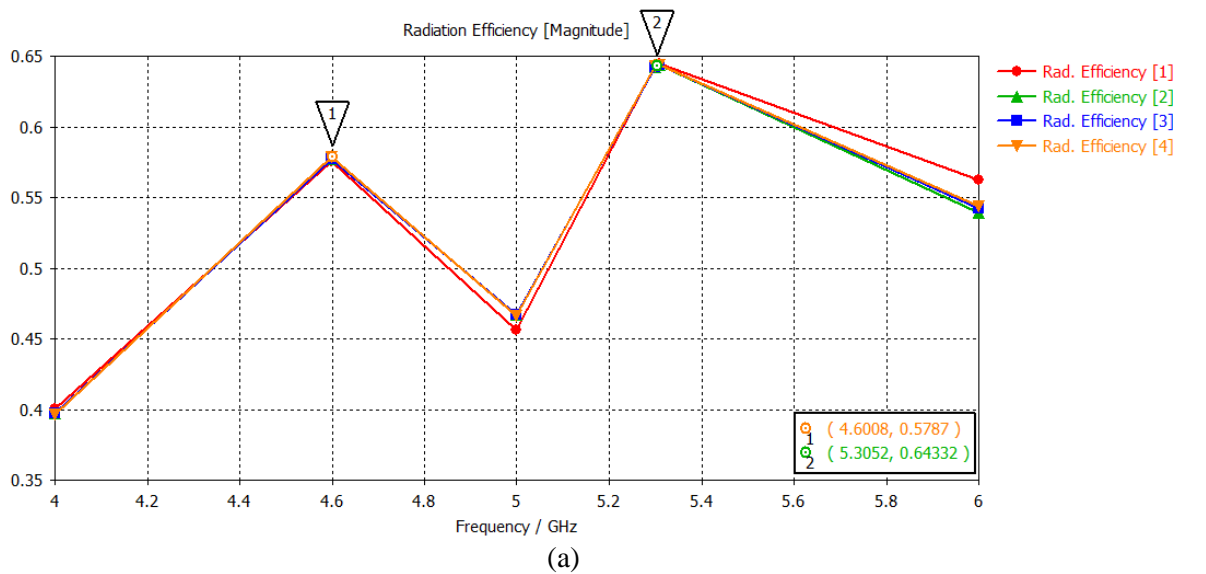
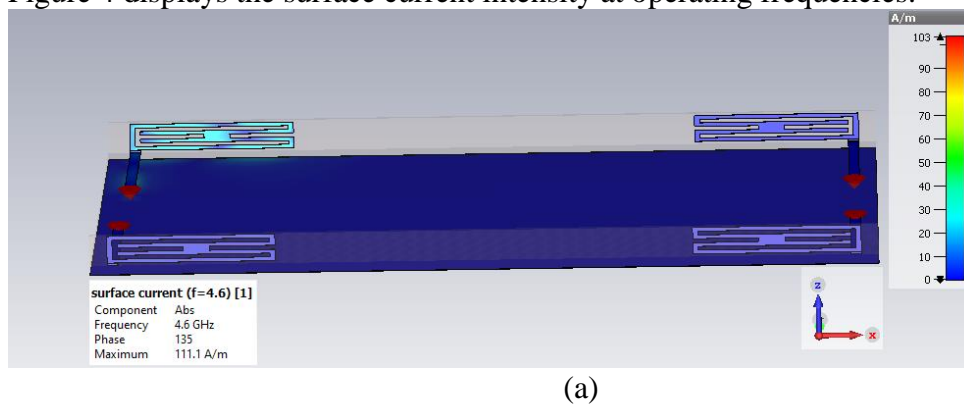
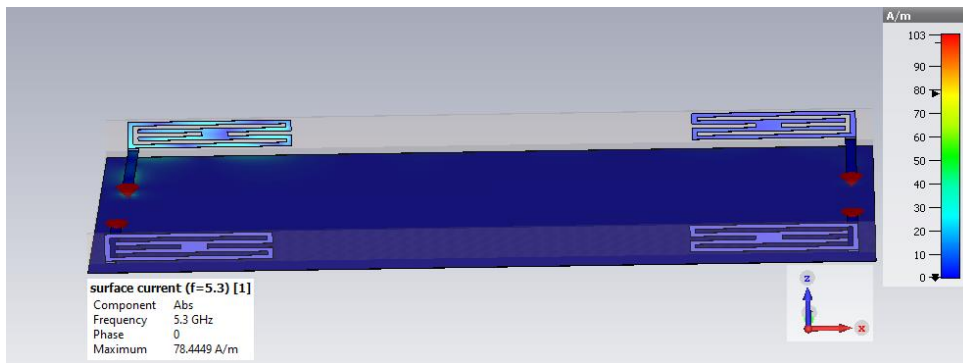


Figure 3: (a) Radiation Efficiency (b) Total Efficiency

4.3 Surface Current Distribution

Figure 4 displays the surface current intensity at operating frequencies.



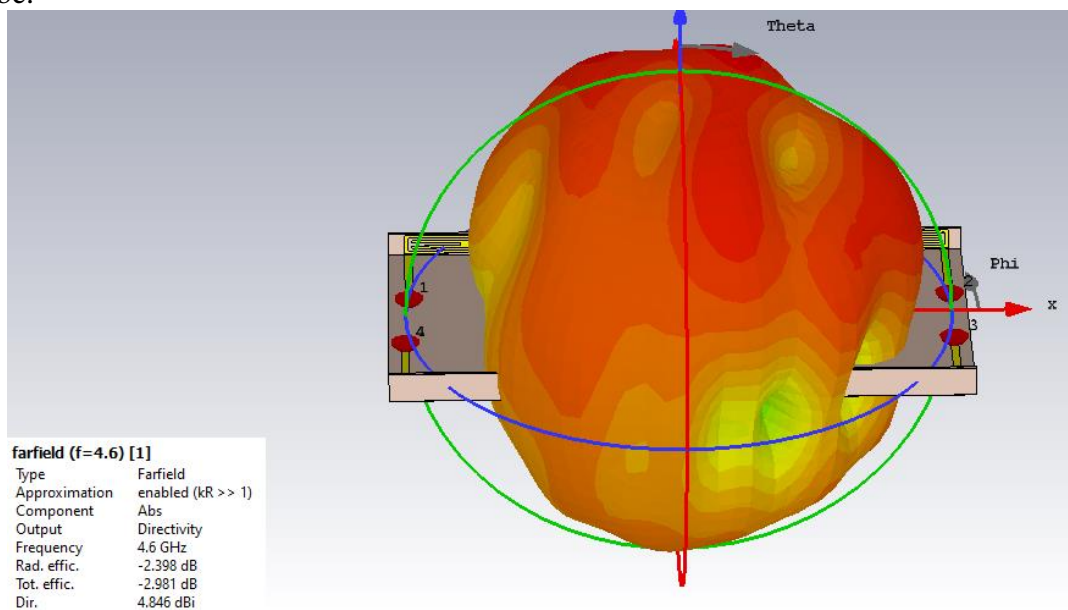


(b)

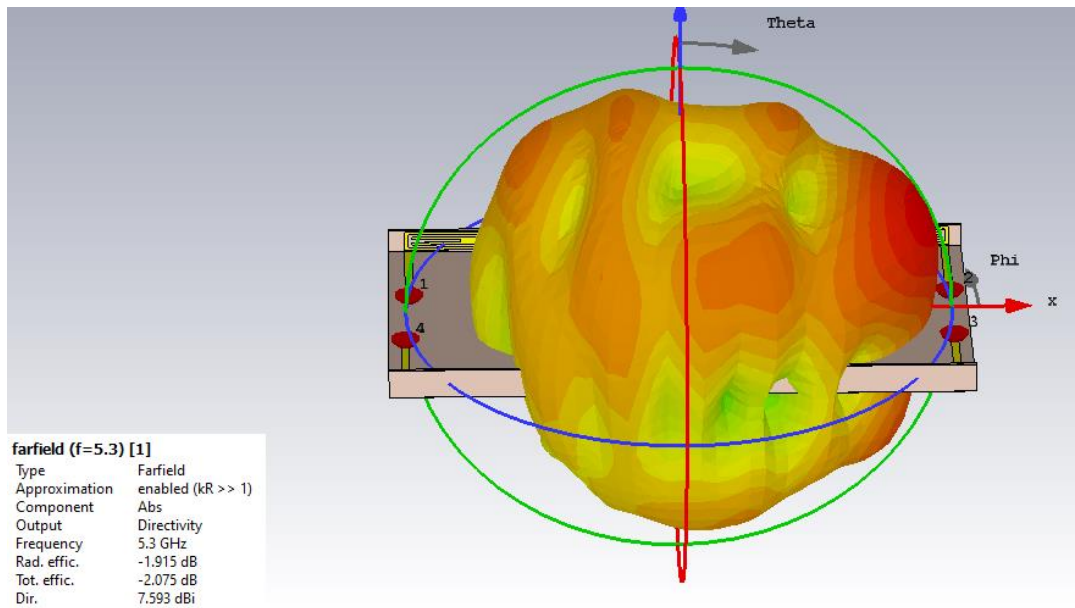
Figure 4: Surface current density (a) at 4.6 GHz (b) 5.3 GHz, when antenna-1 is excited.

4.4 Radiation Pattern

Figure 5 displays the 4.6 GHz and 5.3 GHz radiation parameters of the proposed device. It displays the far-field patterns for the $\theta = 0$ and $\phi = 90$ lines. It is important to observe that the radiating components are arranged on the board to create a system with a wideband, quasi-isotropic general design. In this context, the terms "wideband" and "isotropic" apply to the half-power beam width (HPBW) and, respectively, the uniform distribution of radiation around a spheroid. A maximal directivity of 7.3 dBi is attained when the provided antenna emits the majority of its power in the direction of the main lobe.



(a)



(b)

Figure 4: Radiation Pattern (a) at 4.6 GHz (b) at 5.3 GHz

4.5 MIMO Parameters

In MIMO networks, the Envelope Correlation Coefficient (ECC) is becoming more important. The amount to which the MIMO antenna components affect one another is specified. In other words, there is little to no crosstalk between the radiating components, and better MIMO system efficiency is encouraged by lower ECC.

The ECC was calculated using the radiating components' 3D electric field structures within an array. It is crucial to keep in mind that, when calculating ECC, a uniform incident wave setting is considered. Figure 8 displays the outcome of the ECC. All of the situations considered have an ECC that is significantly lower than 0.04, which is in accordance with global standards for 5G MIMO antenna systems. (ECC 0.5).

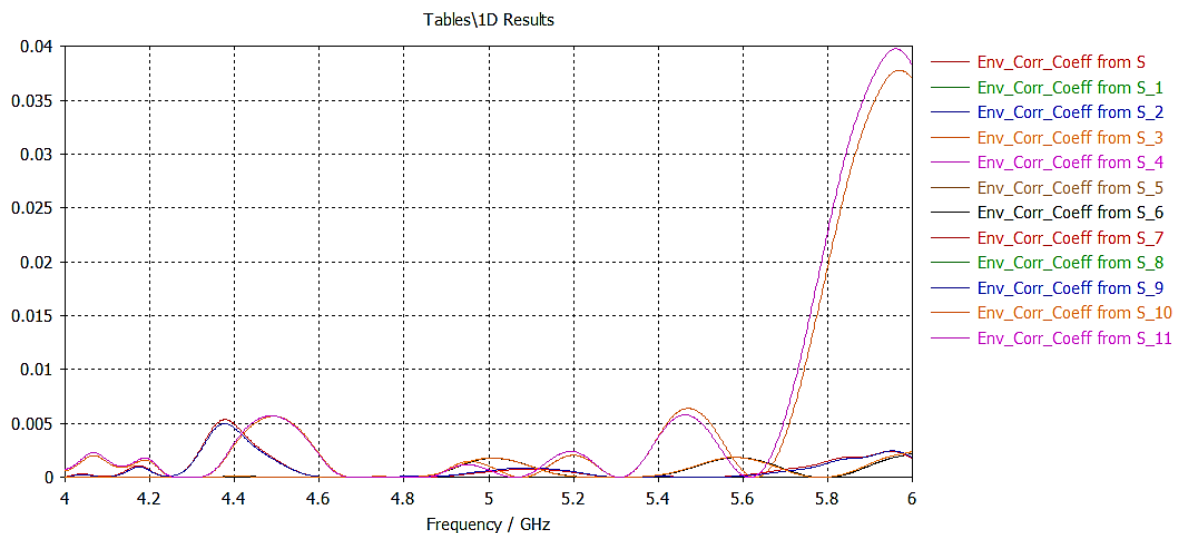


Figure 5: Envelop Correlation Coefficient (ECC)

5 Comparative analysis with published works

Table 1 highlights the variations between the 4-Port 5G MIMO antenna under review and the previous research. It is very obvious that the suggested antenna does not require any extra decoupling methods to serve the 5G New radio LTE Bands 46 and 79. Additionally, there is excellent isolation between resonant components, which lessens the complexity of the design. The obtained envelope correlation coefficient number is also quite low, indicating better diversity performance.

Table -1 A Comparison with published research

Reference	Bandwidth (GHz)	5G Bands	Elements Size	No. of antennas	ECC	Efficiency (%)
Proposed	4.4-5.9 (-10 dB)	n79, LTE Band 46	32*8.25 mm	4	< 0.04	64%
[2]	3.4-3.6 (-10 dB)	Partially n77, n78	21.5 x 3	8	<0.05	62-76
[16]	3.4-3.6 (-10 dB)	Partially n77, n78	14.2 x 9.4	8	<0.2	>40
[15]	3.3-4.2 4.8-5.0	Partially n77, n78,79	49.6*7	8	<0.12	62.6-79.1
[20]	3.4-3.6 (-17 dB)	Partially n77, n78	20*7	4	<0.1	60-72
[21]	3.3-3.6 (-17 dB)	Partially n77, n78	25*7	4	<0.05	56.2-64.7

5. Conclusions

This study's main objective was to propose a simple antenna system that can satisfy 5G technology's criteria in the sub-6 GHz frequency range. A 4-element MIMO antenna device with an H-shaped monopole antenna is demonstrated on a low-cost FR4. The antenna covers the two 5G New Radio bands: n79 (4.4-5 GHz) and LTE Band 46 (5.1-5.9 GHz). A non-ground area approximately 32 mm by 8.25 mm is used to place each antenna. The antennas are strategically placed on the substrate's borders, eliminating the need for any extra decoupling techniques. To allow other RF components and devices, the radiating parts are positioned on the same side of the circuit board. A wide range of significant operational factors are used to evaluate the efficacy of the proposed system. In both frequencies, mutual coupling is significantly below -10 dB. At 5.3 GHz, the maximum gain of 5.6 dB is attained, and at the other frequency, a gain of more than 2.4 dB is attained. The ECC of the MIMO antenna is considerably less than the industry average of 0.04. The provided antenna also provides space for another circuitry that are present inside the mobile terminal due to its small antenna size. It's reasonable to infer that the proposed MIMO system can be used in the future with a range of wireless technologies.

Reference

- [1] M. A. Jensen and J. W. Wallace, "A review of antennas and propagation for MIMO wireless communications," *IEEE Transactions on Antennas and Propagation*, vol. 52, no. 11, pp. 2810–2824, Nov. 2004. doi: 10.1109/TAP.2004.835272.
- [2] Y. Li, C. Y. D. Sim, Y. Luo, and G. Yang, "High-Isolation 3.5 GHz Eight-Antenna MIMO Array Using Balanced Open-Slot Antenna Element for 5G Smartphones," *IEEE Trans Antennas Propag*, vol. 67, no. 6, pp. 3820–3830, Jun. 2019, doi: 10.1109/TAP.2019.2902751.
- [3] A. Zhao and Z. Ren, "Size Reduction of Self-Isolated MIMO Antenna System for 5G Mobile Phone Applications," *IEEE Antennas Wirel Propag Lett*, vol. 18, no. 1, pp. 152–156, Jan. 2019, doi: 10.1109/LAWP.2018.2883428.
- [4] A. Zhao and Z. Ren, "Wideband MIMO antenna systems based on coupled-loop antenna for 5G N77/N78/N79 applications in mobile terminals," *IEEE Access*, vol. 7, pp. 93761–93771, 2019, doi: 10.1109/ACCESS.2019.2913466.
- [5] H. Wang, R. Zhang, Y. Luo, and G. Yang, "Compact eight-element antenna array for triple-band MIMO operation in 5G mobile terminals," *IEEE Access*, vol. 8, pp. 19433–19449, 2020, doi: 10.1109/ACCESS.2020.2967651.
- [6] X. Zhang, Y. Li, W. Wang, and W. Shen, "Ultra-Wideband 8-Port MIMO Antenna Array for 5G Metal-Frame Smartphones," *IEEE Access*, vol. 7, pp. 72273–72282, 2019, doi: 10.1109/ACCESS.2019.2919622.
- [7] C. Y. D. Sim, H. Y. Liu, and C. J. Huang, "Wideband MIMO Antenna Array Design for Future Mobile Devices Operating in the 5G NR Frequency Bands n77/n78/n79 and LTE Band 46," *IEEE Antennas Wirel Propag Lett*, vol. 19, no. 1, pp. 74–78, Jan. 2020, doi: 10.1109/LAWP.2019.2953334.
- [8] Q. Cai, Y. Li, X. Zhang, and W. Shen, "Wideband MIMO Antenna Array Covering 3.3-7.1 GHz for 5G Metal-Rimmed Smartphone Applications," *IEEE Access*, vol. 7, pp. 142070–142084, 2019, doi: 10.1109/ACCESS.2019.2944681.
- [9] H. D. Chen, Y. C. Tsai, C. Y. D. Sim, and C. Kuo, "Broadband Eight-Antenna Array Design for Sub-6 GHz 5G NR Bands Metal-Frame Smartphone Applications," *IEEE Antennas Wirel Propag Lett*, vol. 19, no. 7, pp. 1078–1082, Jul. 2020, doi: 10.1109/LAWP.2020.2988898.
- [10] A. Singh and C. E. Saavedra, "Wide-bandwidth inverted-F stub fed hybrid loop antenna for 5G sub-6 GHz massive MIMO enabled handsets," *IET Microwaves, Antennas and Propagation*, vol. 14, no. 7, pp. 677–683, Jun. 2020, doi: 10.1049/iet-map.2019.0980.
- [11] W. Jiang, B. Liu, Y. Cui, and W. Hu, "High-Isolation Eight-Element MIMO Array for 5G Smartphone Applications," *IEEE Access*, vol. 7, pp. 34104–34112, 2019, doi: 10.1109/ACCESS.2019.2904647.
- [12] J. Guo, L. Cui, C. Li, and B. Sun, "Side-Edge Frame Printed Eight-Port Dual-Band Antenna Array for 5G Smartphone Applications," *IEEE Trans Antennas Propag*, vol. 66, no. 12, pp. 7412–7417, Dec. 2018, doi: 10.1109/TAP.2018.2872130.
- [13] W. Hu *et al.*, "Dual-band eight-element MIMO array using multi-slot decoupling technique for 5G terminals," *IEEE Access*, vol. 7, pp. 153910–153920, 2019, doi: 10.1109/ACCESS.2019.2948639.
- [14] W. Jiang, Y. Cui, B. Liu, W. Hu, and Y. Xi, "A Dual-Band MIMO Antenna with Enhanced Isolation for 5G Smartphone Applications," *IEEE Access*, vol. 7, pp. 112554–112563, 2019, doi: 10.1109/ACCESS.2019.2934892.
- [15] L. Cui, J. Guo, Y. Liu, and C. Y. D. Sim, "An 8-Element dual-band MIMO antenna with decoupling stub for 5G smartphone applications," *IEEE Antennas Wirel*

- Propag Lett*, vol. 18, no. 10, pp. 2095–2099, Oct. 2019, doi: 10.1109/LAWP.2019.2937851.
- [16] L.-Y. Rao and C.-J. Tsai, “8-loop Antenna Array in the 5 Inches Size Smartphone for 5G Communication the 3.4 GHz-3.6 GHz Band MIMO Operation,” 2018.
- [17] L. Yang and T. Li, “Box-folded four-element MIMO antenna system for LTE handsets,” *Electron Lett*, vol. 51, no. 6, pp. 440–441, Mar. 2015, doi: 10.1049/el.2014.3757.
- [18] J. Choi, W. Hwang, C. You, B. Jung, and W. Hong, “Four-Element Reconfigurable Coupled Loop MIMO Antenna Featuring LTE Full-Band Operation for Metallic-Rimmed Smartphone,” *IEEE Trans Antennas Propag*, vol. 67, no. 1, pp. 99–107, Jan. 2019, doi: 10.1109/TAP.2018.2877299.
- [19] M. Abdullah, Y.-L. Ban, K. Kang, M.-Y. Li, and M. Amin, “Eight-Element Antenna Array at 3.5 GHz for MIMO Wireless Application,” 2017.
- [20] Z. Ren, A. Zhao, and S. Wu, “MIMO Antenna With Compact Decoupled Antenna Pairs for 5G Mobile Terminals,” *IEEE Antennas Wirel Propag Lett*, vol. 18, no. 7, pp. 1367–1371, Jul. 2019, doi: 10.1109/LAWP.2019.2916738.
- [21] L. Chang, Y. Yu, K. Wei, and H. Wang, “Polarization-orthogonal co-frequency dual antenna pair suitable for 5G MIMO smartphone with metallic bezels,” *IEEE Trans Antennas Propag*, vol. 67, no. 8, pp. 5212–5220, Aug. 2019, doi: 10.1109/TAP.2019.2913738.